Plant Direct

WILEY

American Society of Plant Biologists SEB SOCIETY FOR EXPERIMENTAL BIOLOGY

RESEARCH ARTICLE OPEN ACCESS

RNA-Binding Proteome-Wide Analysis Reveals Rice RNA-Binding Proteins Enriched After Sobemovirus Rice Yellow Mottle Virus Infection

Patrick Jacob Odongo[1,2] | Roosje Van Ende[1] | Sam Balzarini[1] | Geoffrey Onaga[3] | Titus Alicai[2] | Koen Geuten[1]

[1]Molecular Biotechnology of Plants and Micro-Organisms, Institute of Botany and Microbiology, KU Leuven, Leuven, Belgium | [2]National Crops Resources Research Institute, National Agriculture Research Organization, Kampala, Uganda | [3]Africa Rice Center, Bouake, Cote d'Ivoire

Correspondence: Koen Geuten (koen.geuten@kuleuven.be)

Received: 18 September 2024 | **Revised:** 4 April 2025 | **Accepted:** 17 April 2025

Funding: The VLIR-UOS Support to the Global Minds Scholarship at KU Leuven, Belgium, financially supported this work (BE2017GMUKUA101). The Global Minds Program provided a Ph.D. grant to Patrick Jacob Odongo. Funding organizations did not participate in the design of the study and collection, analysis, and interpretation of data or in writing the manuscript.

Keywords: RBPome | RNA binding proteins | SAPS | Sobemovirus RYMV | susceptibility gene | viruses

ABSTRACT

RNA-binding protein interactions with viral RNA are crucial in the context of viral infections, as viral RNAs can recruit and reprogram host RNA-binding proteins (RBPs) during disease progression. Despite their significance, the repertoire of RBPs involved in most viral infections remains inadequately characterized. In Africa, Sobemovirus Rice yellow mottle virus (Sobemovirus RYMV) is the most prevalent virus infecting rice, and its devastating impact has led to extensive research efforts worldwide. Comprehensive identification of host RBPs that are enriched under Sobemovirus RYMV-infected conditions through RNA-bound proteome (RBPome)-wide studies could provide novel strategies for developing Sobemovirus RYMV resistance. In this study, a silica-based acidic phase separation approach was employed to elucidate changes in the RBPome following Sobemovirus RYMV infection. The analysis demonstrated that Sobemovirus RYMV infection remodels the RBPome, with 11 non-viral RBPs identified as significantly enriched and two non-viral RBPs that were significantly less abundant following infection. This study provides a snapshot of the landscape of RBPome changes in response to Sobemovirus RYMV. Validating these RBPs to understand their biological involvement in Sobemovirus RYMV infection is crucial to developing Sobemovirus RYMV-resistant rice varieties.

1 | Introduction

As obligate organisms, viruses rely on host cells for survival. Due to the limited number of proteins they encode on their own genome, viruses must hijack and reprogram host proteins to support their lifecycle (Nagy and Pogany 2012; Dicker et al. 2021; Davey et al. 2011). Viral and host proteins help to navigate the viral RNA through a series of metabolic pathways, including replication and movement, to ultimately deliver the viral RNA genome into new cells (Dicker et al. 2021; Garcia-Moreno et al. 2019). A key component of these processes is the interaction between viral RNAs and cellular RNA-binding proteins (RBPs), where both viral and cellular proteins play roles in guiding viral RNA metabolism (Dicker et al. 2021; Davey et al. 2011; Girardi et al. 2021).

Generally, to confer resistance against pathogens in plants, typically dominant resistance (R) genes are deployed. However,

Patrick Jacob Odongo and Roosje Van Ende contributed equally.

because R gene-based resistance is often monogenic, these narrow-spectrum genes can be overcome by other pathogens or strains. By contrast, resistance to viruses can also occur through the disruption of proviral factors or susceptibility (S) gene products, leading to incompatible host–virus interactions. These are host proteins that are essential for the viral lifecycle, converting a host cell into a supportive environment for the virus. Recessive (S) resistance is known to provide a more broad-spectrum and durable type of resistance than R-genes (Van Schie and Takken 2014). Host proteins that facilitate different stages of viral infection represent potential targets for virus management. Recent reviews have summarized our current understanding of host proteins that influence susceptibility to plant viruses (Van Schie and Takken 2014; Garcia-Ruiz 2018; Bastet et al. 2017; Mäkinen 2020).

Recently, high-throughput strategies have been established to characterize cellular RBPs involved in viral responses across eukaryotic systems, as highlighted in recent reviews (Van Ende et al. 2020; Gräwe et al. 2021). A prominent example, specifically identifying viral RNA interacting proteins, is RNA antisense purification coupled with mass spectrometry (RAP-MS) (McHugh and Guttman 2018; Lee et al. 2021; Schmidt et al. 2021). Also, more general approaches, studying the whole RNA-binding proteome (RBPome) dynamics after infection, have emerged with the establishment of organic phase separation approaches (Urdaneta and Beckmann 2019; Queiroz et al. 2019; Trendel et al. 2019). Evidence from mammalian viruses, such as Sindbis virus (SINV) (Garcia-Moreno et al. 2019), has shown that viral infection alters the complement of active host RBPs due to variations in RNA availability. However, despite their success in mammalian systems, only a few of these approaches have been applied to viral–plant interactions (Marondedze et al. 2016; Reichel et al. 2016; Köster et al. 2019).

This study employed a silica-based acidic phase separation (SAPS) approach to identify cellular RBPs with dynamic changes and differential RNA-binding activity under healthy and Sobemovirus RYMV-infected conditions. SAPS is an organic phase separation technique that isolates all ultraviolet (UV) crosslinked ribonucleoprotein (RNP) complexes, known as the RBPome, through a combination of silica-based purification of RNA and RNPs, followed by an acid guanidinium thiocyanate-phenol-chloroform (AGPC) extraction, which further separates the RNP complexes (Figure 1) (Balzarini et al. 2023).

Sobemovirus RYMV, endemic to Africa, can cause up to 100% yield loss (Bakker n.d.; Hébrard et al. 2021). Sobemovirus RYMV is a virus with a monopartite-positive RNA strand of approximately 4.5 kb. Its genome contains four open reading frames (ORFs) that encode five proteins (Hébrard et al. 2021; Fargette et al. 2004). Sobemovirus RYMV has stable particles, replicates rapidly, and is found in various intracellular compartments (Opalka et al. 2000). All elite cultivars are susceptible to Sobemovirus RYMV, thus the development of resistant cultivars is the most promising approach. The recessive resistance locus RYMV2 (OsCPR5.1) has been identified in African rice (*Oryza glaberrima*). However, introgression into *Oryza sativa*, the most widely cultivated rice species globally, including its subspecies

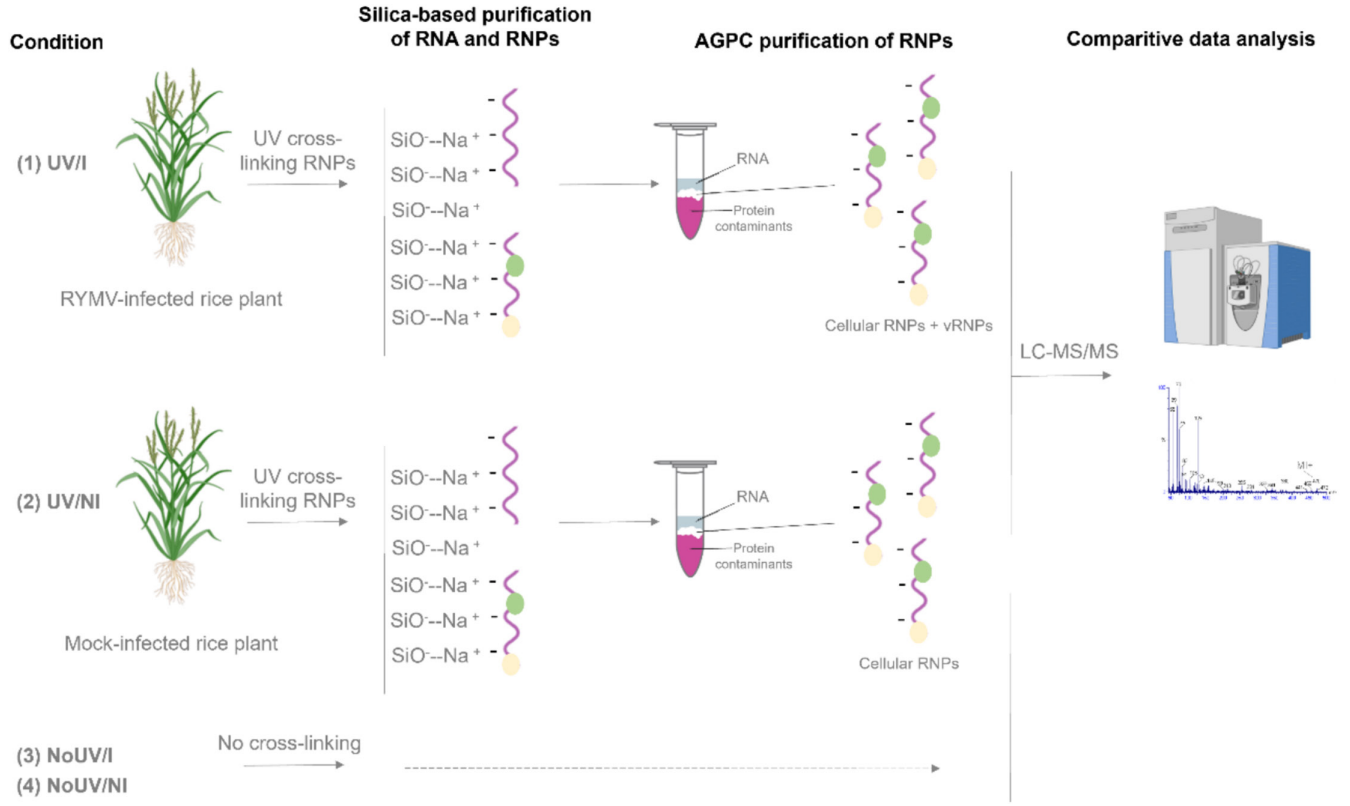

FIGURE 1 | Experimental set-up of the RBPome isolation. RNPs of (1) UV crosslinked Sobemovirus RYMV-infected (UV/I), (2) UV crosslinked non-infected (UV/NI), (3) Non-crosslinked Sobemovirus RYMV-infected (NoUV/I), and (4) non-crosslinked non-infected (NoUV/NI) rice plants are isolated using the SAPS procedure and protein abundances compared using comparative mass spectrometry analysis.

japonica and indica, remains challenging due to crossing barriers between the species (Orjuela et al. 2013; Pidon et al. 2020). Identifying and functionally validating host RBPs required by Sobemovirus RYMV at any stage of its life cycle is a crucial step toward breeding Sobemovirus RYMV-resistant plants.

In this study, over 200 RBPs were identified in the susceptible rice cultivar *O. sativa* indica IR64 under both healthy and Sobemovirus RYMV-infected conditions. Among these, 13 non-viral RBPs showed significant changes in abundance or RNA-binding activity during Sobemovirus RYMV infection (of which 11 significantly enriched and two significantly less abundant in the UV-infected sample). These RBPs are considered potential targets for functional validation of their roles in Sobemovirus RYMV infection and for resistance breeding. The findings of this study may provide a foundation for profiling key RBPs involved in the life cycle of other plant viruses.

2 | Results

2.1 | Determining the Optimal Time Point for Sample Harvest

To determine the time point for harvesting, susceptible rice cultivar IR64 was inoculated with Sobemovirus RYMV at 21 days post-seeding. Leave samples were collected at 2, 4, 6, 8, 10, 12, and 14 days post-inoculation (dpi) for the quantification of the viral load using RT-qPCR. Systemic infection was detected from 4 dpi in newly emerged leaves. Viral RNA levels increased exponentially starting at 8 dpi, peaking at 10 dpi, and then declining post-10 dpi, (Figure 2a) coinciding with the onset of severe symptoms indicating the initiation of cell death in the infected leaf. Leaves harvested at 2 and 4 dpi showed no typical Sobemovirus RYMV symptoms, while leaves at 7 dpi were green but with dots or streaks. At 12 and 14 dpi, leaves showed yellow streaking and mottling (Figure 2b). Based on these observations, 8 dpi was selected as the optimal harvest time point. At this stage, viral titers were consistently high across all leaf samples with minimal symptom development.

2.2 | UV Crosslinking RNP Complexes

To evaluate the efficiency and specificity of the SAPS protocol in isolating RBPs over non-crosslinked proteins in rice, a range of UV crosslinking conditions were compared against a non-crosslinked control. One gram of liquid nitrogen flash-frozen leaf powder was treated with UV doses of 2.5, 4, and 6 J/cm^2. Following the SAPS procedure, proteins were visualized using silver stain gel. As anticipated, the non-crosslinked control exhibited minimal protein isolation, while increasing doses of UV light were expected to enhance RBP isolation (Figure 3). This indicates the specificity of the procedure to isolate RNPs over non-crosslinked molecules. Based on these results, a treatment with a UV dose of 4 J/cm^2 was determined as sufficient for crosslinking grinded rice leaves in this study.

2.3 | SAPS Reveals an RNA-Binding Proteome Enriched in Sobemovirus RYMV-Infected Rice Leaves

As was proven the SAPS protocol to successfully isolate RBPs over non-crosslinked proteins in rice, the procedure was used to identify the RBPs playing a role in Sobemovirus RYMV-infected plants. Four experimental conditions were analyzed and compared: (1) UV crosslinked and Sobemovirus RYMV-infected (UV/I), (2) UV crosslinked and non-infected (UV/NI), (3) non-crosslinked and Sobemovirus RYMV-infected (NoUV/I), and (4) non-crosslinked and non-infected (NoUV/NI). Each condition included five biological replicates. Principal component analysis demonstrated a strong correlation within each group, indicating high reproducibility of the replicates (Figure 4).

A total of 306 protein groups were reliably quantified, defined as protein groups with at least three valid label-free quantification intensity values in one of the experimental conditions. Comparisons between the experimental conditions yielded the following results (significance is considered if FDR < 0.05, logFC > |2|):

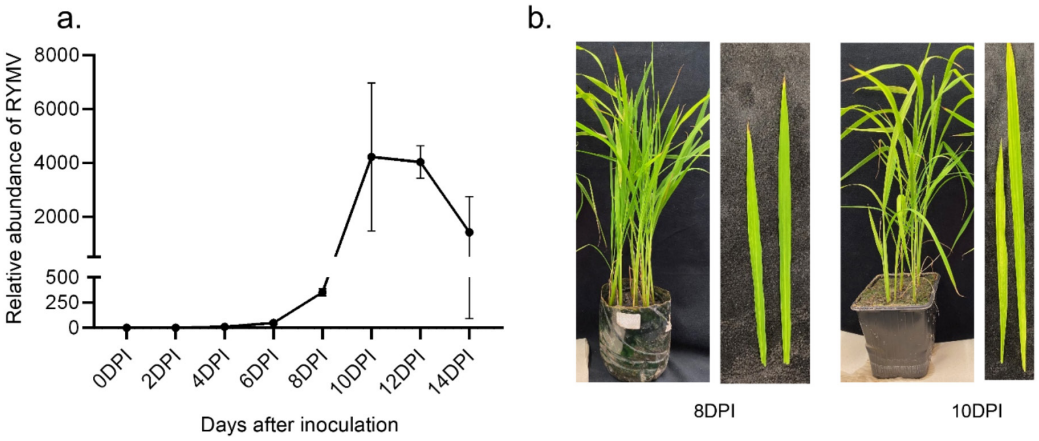

FIGURE 2 | Sobemovirus RYMV infection profile (a.) Relative expression of Sobemovirus RYMV in the infected IR64 variety. Three plants (biological replicates) were planted for each time point, and all the leaves were mechanically inoculated with the UG01 Sobemovirus RYMV isolate 21 days after sowing. Only newly emerged leaves (systemic leaves) were harvested for expression analysis at each time point. Local infection titers were not taken. Error bars represent standard deviation. Data was normalized to 18S ribosomal RNA endogenous control (dpi, days post-inoculation). (b.) Phenotype of Sobemovirus RYMV-infected plants at 8 dpi and 10 dpi.

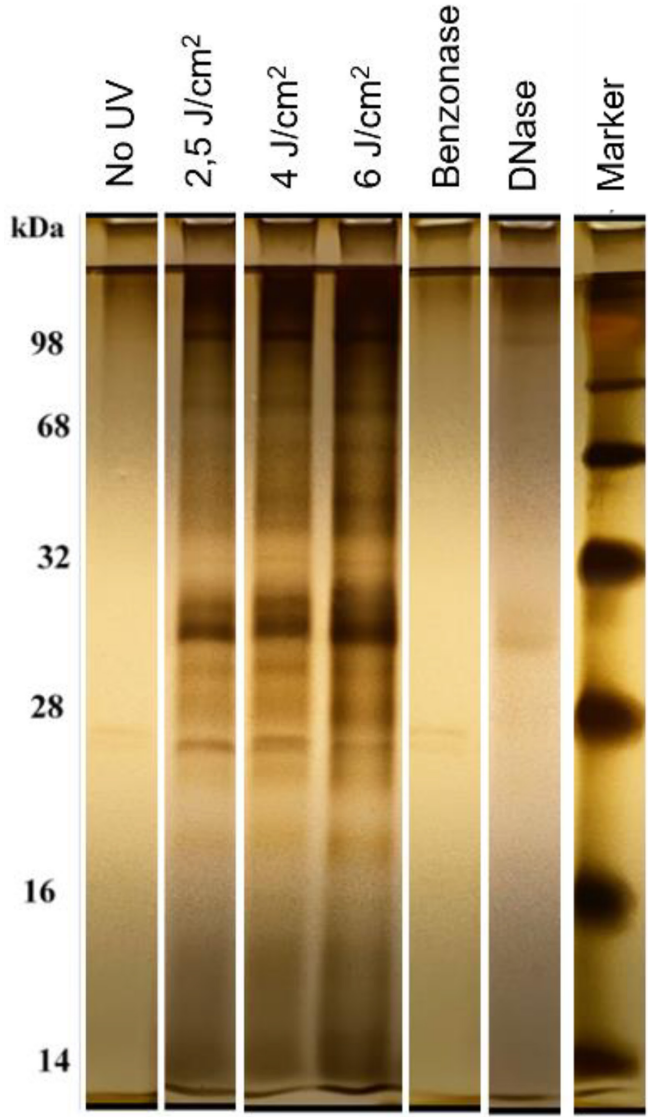

FIGURE 3 | RBPome visualization of rice plants under different UV doses. The proteins were visualized in silver stain after the acidic phenol:chloroform separation step. Benzonase and DNase are added as a control (only these enzymes loaded, not a sample treated with). A Benzonase treatment is performed before silver stain analysis, a DNase treatment is included in the SAPS protocol to remove residual DNA.

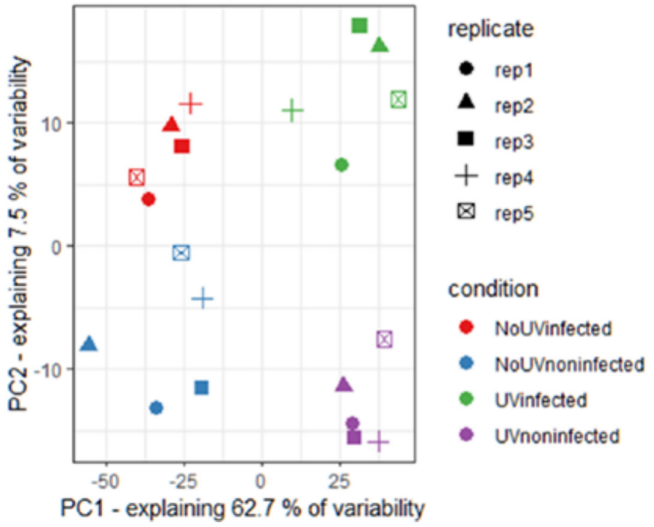

FIGURE 4 | Scatter plot showing sample mapping along two principal components (PCs). The percentages of the explained data variance for each PC are shown on the x- and y-axes.

a. UV/NI vs. NoUV/NI (Condition 2 vs. Condition 4): 175 proteins were significantly enriched and 1 protein was significantly less abundant in the UV/NI sample compared to the NoUV/NI sample (Figure 5a). Theoretically, this is the "steady-state" rice RBPome.

b. UV/I vs. NoUV/I (Condition 1 vs. Condition 3): 217 proteins were significantly enriched in the UV/I sample compared to the NoUV/I sample (Figure 5b). Theoretically, this is the "steady-state" rice RBPome after infection with Sobemovirus RYMV.

c. NoUV/I vs. NoUV/NI (Condition 3 vs. Condition 4): Comparison showed two proteins significantly enriched and one protein significantly less abundant in the NoUV/I sample compared to the NoUV/NI sample (Figure 5c).

d. UV/I vs. UV/NI (Condition 1 vs. Condition 2): This comparison indicated that 15 proteins were significantly enriched and four proteins were significantly less abundant in the UV/I sample compared to the UV/NI sample (Figure 5d). Theoretically, these are RBPs specifically altered in abundance or RNA-binding activity after Sobemovirus RYMV-infection, making them of particular interest. These RBPs were referred to as candidate RBPs, which could be involved in Sobemovirus RYMV infections. As expected, three viral proteins are significantly enriched in the UV/I samples. These proteins are shown in Table 1 with the respective adjusted *p* value and logFC for all four comparisons.

For all of these comparisons, the Venn diagram is depicted in Figure 5.

3 | Discussion

Plant susceptibility to viruses is influenced by the presence of host proteins that can facilitate the infection. Consequently, disrupting the interactions with these host molecules co-opted by the virus can significantly impact the viral life cycle (Van Schie and Takken 2014; Garcia-Ruiz 2018). As shown by Garcia-Moreno et al. (2019), RBPs altered after infection could be crucial for viral infection efficacy. Based on this, RBPs that are significantly altered during Sobemovirus RYMV infection were profiled. For this purpose, the SAPS protocol for RBPome isolation previously used in Arabidopis was utilized (Balzarini et al. 2023).

An early stage of Sobemovirus RYMV infection (8 dpi) was selected for harvesting systemically infected leaf samples for and UV crosslinking (Figure 1). This time point was chosen to balance quantifiable viral titer with limited secondary effects (symptom development and defense pathways). These could dominate the infected RBPome, however, less useful for combating the virus. We hypothesized that at this period, the isolated RBPs will be a mix of genes important early in infection and genes involved in later

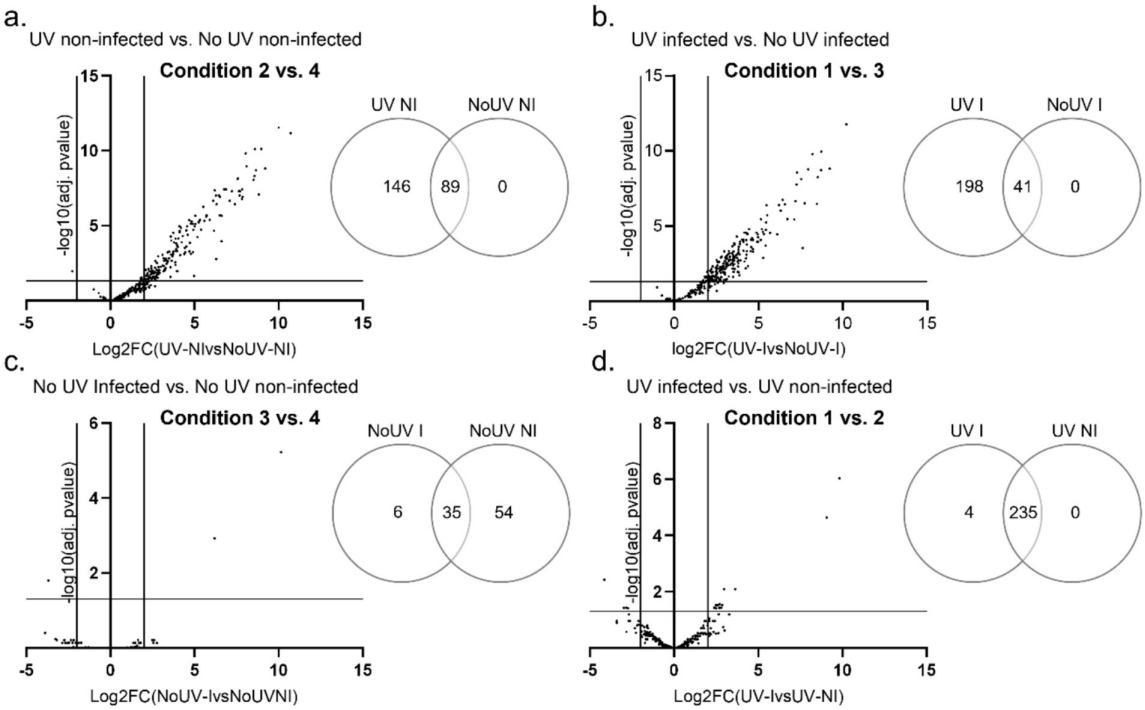

FIGURE 5 | Analysis of the RBPome in Sobemovirus RYMV-infected and non-infected IR64 rice cultivar. (a–d) Volcano plot showing the log2 fold enrichment and significance (adjusted *p*-value) of each protein. Venn diagrams showing unique and overlapping proteins between, (a) UV crosslinked and non-infected vs. non-crosslinked and non-infected, (b) UV crosslinked and Sobemovirus RYMV-infected vs. non-crosslinked and Sobemovirus RYMV-infected, (c) non-crosslinked and Sobemovirus RYMV-infected vs. non-crosslinked and non-infected, and (d) UV crosslinked and Sobemovirus RYMV-infected vs. UV crosslinked and non-infected. Significant proteins are shown in the upper right and left quadrants (FDR < 0.05, logFC > |2|), $n = 5$.

stages. In follow-up experiments, it could be interesting to compare the RBPs isolated at 8 dpi with earlier and later time points to map proteins involved in all stages of the viral life cycle. Our specific interest was to find dynamic changes of the RBPome in the earlier stages of infection, as these can be more promising targets for loss-of function-based resistance (Van Schie and Takken 2014).

The procedure for RBPome isolation (SAPS) was initially applied to Arabidopsis by Balzarini et al. (2023). This study represents the first application of the SAPS technique to rice. To confirm the specific isolation of RBPs, the protein content of a UV crosslinked sample with a non-crosslinked sample after SAPS was compared. Following SAPS, performed under denaturing conditions, only the crosslinked complexes consisting of both RNA and proteins should remain due to their covalent link. The results in this study confirmed the applicability of SAPS to rice, as the non-crosslinked sample appears 'nearly empty' on silver stain. Additionally, the intensity of the protein bands increases upon increasing doses of UV. While it might seem logical to opt for the highest dose of UV light, correlating to the increased RBP abundance, excessively high UV doses are known to cause unintended protein–protein and protein–DNA interactions (Beckmann 2017; Hafner et al. 2010).

Additionally, overexposure to UV light can modify the proteins leaving them unidentifiable by mass spectrometry (Wagenmakers et al. 1980). Therefore, a dose of 4 J/cm^2 to balance efficient RBP purification while minimizing potential artifacts was selected. Importantly, in this study, frozen powder was crosslinked unlike many studies that describe crosslinking leaf tissue. This approach partially addresses the issue of limited penetration depth inherent to UV crosslinking plant tissues, ensuring more uniform and effective interaction between the UV light and all layers of the sample (Balzarini et al. 2023; Urdaneta et al. 2019).

Before studying the altered dynamics after Sobemovirus RYMV infection, the RBPome of rice, both with (Condition 1 vs. Condition 3, Figure 5b) and without infection (Condition 2 vs. Condition 4, Figure 5a) was determined. As expected, the Venn diagram shows no proteins unique to the non-crosslinked conditions. The proteins shared between crosslinked and non-crosslinked are either contaminating proteins or highly abundant true RBPs and therefore 'contaminating' the non-crosslinked control. Statistical analysis distinguishes these. As contamination is expected to be equal in both conditions, whereas true RBPs should be enriched in the crosslinked sample even when also identified in the non-crosslinked control.

After establishing the "steady-state" RBPomes both with and without infection, we were particularly interested in the changes between both caused by the viral infection (Condition 1 vs. Condition 2, Figure 5d). As was shown in the Venn Diagram, it is not surprising that the majority of the proteins are shared between conditions, as we anticipated that the RBPome composition remains largely unchanged while its dynamics shift, leading to certain RBPs becoming more abundant than others. The comparative analysis revealed significant enrichment of three viral proteins: viral genome-linked protein (VPg), coat protein (CP), and RNA-directed RNA polymerase (RdRp).

TABLE 1 | Overview of proteins significantly enriched/less abundant in UV/I vs. UV/NI if (FDR < 0.05, logFC > |2|) and their adjusted *p*-value and LogFC for all comparisons. Green—significantly enriched; orange—significantly less abundant, gray—not significant. Protein names highlighted in gray are excluded from the list (see Discussion).

			UV/I[1] vs. UV/NI[2]		UV/NI[2] vs. NoUV/NI[4]		UV/I[1] vs. NoUV/I[3]		NoUV/I[3] vs. NoUV/NI[4]	
			Condition 1 vs. 2		Condition 2 vs. 4		Condition 1 vs. 3		Condition 3 vs. 4	
Protein name	**Majority protein IDs**	**Viral vs. host-derived proteins**	**Adj. *p* value**	**LogFC**	**Adj. *p* value**	**LogFC**	**Adj. *p* value**	**LogFC**	**Adj. *p* value**	**LogFC**
Significantly enriched in UV/I vs. UV/NI										
Capsid protein	A0A097ETC1	Viral protein	0.00000092	9.82	0.98	−0.03	0.0072	3.59	0.0012	6.2
RNA-directed RNA polymerase; RNA-directed RNA polymerase (Fragment);	A0A2I6SDA9	Viral protein	0.000023	9.06	0.68	0.6	0.72	−0.48	0.000006	10.14
N-terminal protein; VPg protein (Fragment); Genome-linked viral protein (Fragment)	A0A097ETA3	Viral protein	0.0081	3.63	0.74	0.3	0.0012	3.29	0.99	0.64
UBC core domain-containing protein	A2WK64	Host protein	0.0081	2.97	0.97	−0.04	0.0048	2.27	0.99	0.66
Eukaryotic translation initiation factor 3 subunit G	B8AE20	Host protein	0.03	2.86	0.14	1.27	0.000079	4.08	0.99	0.06
40S ribosomal protein S19	A2XI59; A6MZL9; B8AK61	Host protein	0.037	2.79	0.3	0.96	0.00079	3.47	0.99	0.28
RRM domain-containing protein	B8B413	Host protein	0.037	2.72	0.27	0.99	0.00024	3.83	0.99	−0.12
DNA topoisomerase type IA zn finger domain-containing protein	B8B0L5	Host protein	0.028	2.71	0.59	0.43	0.0095	2.13	0.97	1.02
Clu domain-containing protein	A2X335	Host protein	0.036	2.68	0.56	0.51	0.00068	3.25	0.99	−0.06

(Continues)

TABLE 1 | (Continued)

			UV/I[1] vs. UV/NI[2]		UV/NI[2] vs. NoUV/NI[4]		UV/I[1] vs. NoUV/I[3]		NoUV/I[3] vs. NoUV/NI[4]	
			Condition 1 vs. 2		Condition 2 vs. 4		Condition 1 vs. 3		Condition 3 vs. 4	
Protein name	**Majority protein IDs**	**Viral vs. host-derived proteins**	**Adj. *p* value**	**LogFC**	**Adj. *p* value**	**LogFC**	**Adj. *p* value**	**LogFC**	**Adj. *p* value**	**LogFC**
KH_dom_type_1 domain-containing protein	B8AF48	Host protein	0.039	2.67	0.11	1.49	0.000085	4.27	0.99	−0.11
Ribonuclease	A2X5H4	Host protein	0.03	2.58	0.66	−0.35	0.0025	2.57	0.99	−0.34
Transcription factor GTE4	B8AAI9	Host protein	0.039	2.49	0.7	−0.32	0.006	2.45	0.99	−0.28
C3H1-type domain-containing protein	B8AC88	Host protein	0.03	2.48	0.45	0.56	0.0005	2.97	0.99	0.08
RRM domain-containing protein	B8B8K2	Host protein	0.037	2.43	0.34	0.76	0.024	1.81	0.74	1.37
PWWP domain-containing protein	B8AZ10	Host protein	0.037	2.38	0.65	0.36	0.0012	2.76	0.99	−0.02
Significantly less abundant in UV/I vs. UV/NI										
40S ribosomal protein S7; 40S ribosomal protein S7 (Fragment)	A2XFL8	Host protein	0.039	−2.73	4.3E−06	5.33	0.0052	2.73	0.99	−0.14
KOW domain-containing protein	B8B1V3	Host protein	0.037	−2.84	0.000011	5	0.23	1.05	0.99	1.11
RRM domain-containing protein	A2YIB7	Host protein	0.038	−2.98	3.8E−08	7.83	0.000085	4.66	0.99	0.18
Ribulose bisphosphate carboxylase small subunit; Ribulose bisphosphate carboxylase small subunit (Fragment)	A6N0B6; A6N149; A6N165	Host protein	0.0038	−4.14	0.079	1.71	0.17	1.25	0.016	−3.68

[1]UV crosslinked and Sobemovirus RYMV-infected (UV/I), [2]UV crosslinked and non-infected (UV/NI), [3]non-crosslinked and Sobemovirus RYMV-infected (NoUV/I), and [4]non-crosslinked and non-infected (NoUV/NI).

Sobemovirus RYMV is cap-independent, and VPg is located at the 5′ terminus of ORF1 and is expressed as a polyprotein of ORF2a (Yassi et al. 1994). It has been demonstrated that VPg is a virulence factor for Sobemovirus RYMV and physically interacts with the central domain of eIF (iso)4G1 (Hébrard et al. 2008; Hébrard et al. 2010). CP is essential for the infectivity and cell-to-cell spread of Sobemovirus RYMV infection (Opalka et al. 1998; Bonneau et al. 1998). These viral proteins have been observed to interact with both viral and cellular RNA, promoting Sobemovirus RYMV infection. Although the RdRp is also described to bind RNA and is consequently expected to be present in the "steady-state" infected RBPome (Condition 1 vs. Condition 3), it was surprisingly not significantly enriched in this comparison. One possible hypothesis for this discrepancy is that RdRp might not be cleared from the interphase in the non-crosslinked condition. As the RdRp is unlikely to be a glycoprotein, no immediate explanation for this observation is apparent. To reliably identify the changes in the RBPome after infection (Condition 1 vs. Condition 2), proteins not enriched in the infected RBPome (Condition 1 vs. Condition 3) were excluded from the list. In addition to the RNA-directed RNA polymerase these included the following: RRM domain-containing protein B8B8K2, KOW domain-containing protein B8B1V3 and Ribulose bisphosphate carboxylase small subunit A6N0B6 A6N149, A6N165.

After this exclusion, 11 non-viral RBPs were identified as significantly enriched, while two were found to be significantly less abundant in UV-infected samples (Table 1). Notably, the enriched proteins included eukaryotic translation initiation factor 3 G (eIF3G) and transcription factor GTE4, along with ubiquitin-conjugating enzyme E2, RNA recognition motif (RRM)-containing proteins, K homology domain-containing proteins, and C3H1-type domain-containing proteins. A literature search on other plant viruses was conducted to assess the functional significance of the candidate host RBPs in Sobemovirus RYMV infection. Comparing the candidate RBPs in this study with those implicated in other viral infections suggests potential roles as antiviral or proviral factors in plants.

Eukaryotic translation initiation factor 3 G (eIF3G) is an RNA-binding component of the eIF-3 complex, essential for multiple steps in initiating protein synthesis in eukaryotes (Raabe et al. 2019; Masutani et al. 2007). Plant viruses are known to target eukaryotic translation initiation factors to facilitate their replication. Previous studies have shown that eIF3G is involved in the termination and re-initiation of downstream ORFs in polycistronic viral mRNAs (Schepetilnikov et al. 2011; Fraser and Doudna 2007). The translation re-initiation mechanism of cauliflower mosaic virus (CaMV) and other para-retroviruses has been linked to eIF3. CaMV employs a virus-activated re-initiation mechanism dependent on the p6 protein transactivator viroplasmin (TVA) (Thiébeauld et al. 2009). TVA recruits the re-initiation supporting protein (RISP) to enhance its interaction with eIF3 and 60S ribosomal subunits, thereby accelerating translation re-initiation. Moreover, papaya eIF3G (CpeIF3G) has been shown to interact with the nuclear inclusion protein (NIa) of papaya ring spot virus (PRSV). The C-terminal region of PRSV NIa-proteinase recruits CpeIF3G for translation in papaya mesophyll protoplasts (Gao et al. 2012). The identification of eIF3G in this study is particularly noteworthy, as eIF4G has previously been considered the most critical translation initiation factor in the rice–Sobemovirus RYMV interaction (Albar et al. 2006).

As a member of the bromodomain proteins, general transcription factor group E 4 (GTE4)-bromodomain-containing proteins are promising candidate RBPs involved in viral infection. GTE4 is a bromodomain protein (Brd) characterized by the presence of a bromodomain and an extra-terminal domain (BET). Bromodomain-containing proteins play essential roles in viral multiplication (Hyodo et al. 2014). Previous reports have indicated that potato spindle tuber viroid RNA, a plant subviral pathogen, recruits the bromodomain-containing host protein (BRP1), which is necessary for the nuclear transportation and multiplication of viroid satellite RNA (Martínez de Alba et al. 2003; Chaturvedi et al. 2014). Additionally, another tomato protein, BRP1, interacts with and modulates the nuclear import of the cucumber mosaic virus satellite RNA (Chaturvedi et al. 2014). Although Sobemovirus RYMV has no nuclear phase in its replication cycles, this suggests that GTE4-bromodomain-containing protein might function as a novel RBP.

SAPS also revealed a ubiquitin-conjugating (UBC) core domain-containing protein, ubiquitin-conjugating enzyme E2. The post-translational modification of proteins by ubiquitin or related molecules is a primary regulatory process in virtually all aspects of cell biology (Hyodo et al. 2014; Huh and Paek 2013). Among the three classes of enzymes in the ubiquitin-proteasome system, E2 enzymes are essential for regulating the fate and function of target proteins (Swatek and Komander 2016). Increasing evidence suggests that ubiquitin-conjugating enzymes play both antiviral and proviral roles by degrading viral and cellular proteins, respectively (Alcaide-Loridan and Jupin 2012; Shen et al. 2016; Verchot 2016). For example, proteasome enzymes negatively affect Tobacco mosaic virus and Turnip yellow mosaic virus pathogenesis by degrading the movement protein using the 26S proteasome as a plant defense response (Reichel and Beachy 2000; Drugeon and Jupin 2002). However, other plant viruses use E2 enzymes to assist in viral infection and replication. For example, two tomato E2 proteins (Cdc34p and Ubc2/RAD6) interact with tombusvirus p33 replication protein complexes (Imura et al. 2015; Li et al. 2008). This is an interesting observation because the capsid structure of the family Tombusviridae is related to the Sobemovirus genus, to which Sobemovirus RYMV belongs. Thus, the E2 proteins might be involved in capsid-viral RNA assembly into virions facilitating replication processes (Walker et al. 2021).

RNA recognition motif (RRM) and K homology (KH) domain-containing proteins were also identified. RRM and KH are two of the most common RNA-binding domains involved in transcriptional gene expression in eukaryotes. Notably is that 75% and over 80% of the predicted KH domain and RRM domain-containing proteins have been experimentally determined in plants following genome-wide analysis (LorkoviM 2002; Maris et al. 2005; Cléry et al. 2008). Some human-infecting viruses have been reported to use RRM proteins and KH-domain to support their infection cycle (Darai et al. 2022; Walter et al. 2002).

Although counterintuitively, less abundant proteins in the altered rice RBPome (Condition 1 vs. Condition 2) could also

provide valuable insights. Proteins involved in pathogen defense, for example, might be targeted for degradation in the presence of the virus. Alternatively, an RBP in the rice RBPome could be redirected to support viral metabolism, functioning in alternative roles such as protein–protein interactions, which by consequence would lead to their apparent downregulation. These cases, however, are expected to be exceptions rather than the norm (Dubois et al. 2019).

As presented in Table 1, all RBPs identified as significantly altered after viral infection (Condition 1 vs. Condition 2) are not classified as RBPs in the "steady-state" rice RBPome without infection (Condition 2 vs. Condition 4). One potential explanation, as described by Garcia-Moreno et al. (2019), is that "dormant" RBPs could be "awakened" upon recognizing specific viral signatures within the viral RNA, or their RNA-binding activity may change due to altered RNA availability during infection. However, this observation remains surprising and unexpected. An alternative explanation could include a reduced quality of the sample data of the rice RBPome without infection. This underscores the importance of further validating this dataset to determine which RNAs they are interacting with. For this purpose, an RNA immunoprecipitation assay could be performed. It is important to note, however, that for RBPs to be significantly enriched in these datasets and play a role in infection, direct binding to viral RNA is not strictly necessary. Given that viral RNA becomes the most abundant RNA species during infection, it is plausible to hypothesize that some of these RBPs might indeed physically interact with viral RNA. As a follow-up experiment, knockout lines of these RBPs could be generated and the consequential effect on viral infections quantified.

The non-crosslinked conditions (Conditions 3 and 4) were expected to be "empty" or, at the very least, represent a similar subset of contaminants. The Venn diagram indeed shows an overlap between both non-crosslinked conditions, yet more proteins are present in the non-infected (NI) sample. This could suggest that although the same or similar proteins are expected in the infected (I) sample, their lower abundance might have hindered their identification. However, when considering significance, there was no notable enrichment of proteins in Condition 4 when compared with Condition 3, except for one protein: ribulose bisphosphate carboxylase small subunit. The enrichment of viral proteins in Condition 3 is likely due to their high abundance in the infected sample. Nevertheless, their enrichment in the altered RBPome indicates their potential as RBPs.

In conclusion, S genes enable the establishment of plant virus infection, and their inactivation could provide opportunities for Sobemovirus RYMV resistance breeding in rice. Impairment of these proteins offers an alternative providing rice plants with recessive resistance that is known to be more durable (Hébrard et al. 2010; Opalka et al. 1998). This study identified 11 non-viral RBPs with significantly altered abundance after Sobemovirus RYMV infection. Validating their potential to confer loss-of-susceptibility resistance to Sobemovirus RYMV pathogenicity would be a valuable area of investigation. However, it is important to note that host RBPs play essential endogenous roles, and the loss of S gene function may lead to pleiotropic effects on the plant. Therefore, significant biological challenges must be addressed to fully harness S genes for durable and broad-spectrum resistance to Sobemovirus RYMV (Van Schie and Takken 2014; Garcia-Ruiz 2018).

4 | Materials and Method

4.1 | Plant Growth and Inoculation

Rice seeds were soaked in water for 48 h before being incubated for 24 h at room temperature. Pots measuring 9 × 9 × 10 cm were filled with a 3:1 per volume mixture of sand and superior substrate soil (peltracom) mixed with 0.1 g of iron (111) sulfate heptahydrate. Before seeding, the soil surface was saturated with water, and 10 seeds were planted per pot. The pot was covered with a plastic bag, which was removed after 3 days. The seedlings were transferred to a growth chamber (250 mol/m2s, 16 h/8 h,26°C) and the seedlings were watered for 21 days.

Twenty-one days after sowing (DAS), 10 plants were mechanically inoculated with Sobemovirus RYMV isolate from Uganda (KM487713.1) following the protocol by Pinel-Galzi et al. (2018). Ten plants were mock-inoculated with water and managed in a separate growth chamber having same conditions as described above. Eight days post inoculation (DPI), newly emerged leaves from 10 plants (for both Sobemovirus RYMV infected and mock-inoculated) were harvested. Leaves from two seedlings were pooled together and used as one replicate. All harvested leaves were flash-frozen in liquid nitrogen and stored at −80°C until later use.

4.2 | Determining the Optimal Time Point for UV Crosslinking

Newly emerged leaves were harvested at various time points between 2 and 14 dpi ($n = 5$). Virus expression was quantified by RT-qPCR according to the protocol of the manufacturer (Table 2) (SensiFast SYBR Hi-Rox Kit, GC Biotech).

TABLE 2 | Primers used in this study.

Gene		Primer
18S ribosomal RNA	Forward	5′-CGGCGGATGTTGCTTATAGGAC-3′
	Reverse	5′-GGACCATTCAATCGGTAGGAG-3′
RYMV coat protein	Forward	5′-CAAAGATGGCCAGGAA-3′
	Reverse	5′-CTCCCCCACCCATCCCGAGAATT-3′

4.3 | UV Crosslinking

For UV light crosslinking, a UV crosslinker with a 254-nm UV bulb in the UVP crosslinker (Analytik Jena) was used. Frozen rice leaves (−80°C) were pulverized in liquid nitrogen using a mortar and pestle. Leaf powder (0.5 g) was mixed with liquid nitrogen in a square Petri dish (12 × 12 cm). The Petri dish was placed in liquid nitrogen 7 cm from the bulbs. A dose of 4 J/cm^2 UV light was administered to the powder with pausing and cooling of the sample every 0.5 J/cm^2. The following treatments were applied: (1) UV crosslinked and Sobemovirus RYMV-infected (UV/I), (2) UV crosslinked and non-infected (UV/NI), (3) non-crosslinked and Sobemovirus RYMV-infected (NoUV/I), and (4) non-crosslinked and non-infected (NoUV/NI). After UV crosslinking, the frozen powder was stored at −80°C.

4.4 | RBPome Isolation Using Silica-Based Acid Phase Separation

The RBPome of all four conditions was isolated using the SAPS protocol as described by Balzarini et al. (2023).

4.5 | Silver Staining

After isolation, 10 μL of the SAPS eluate (10%) was incubated for 1 h at 37°C with 0.5 μL of Benzonase. The silver staining assay was performed according to the manufacturer's instructions (Pierce™ Silver Stain Kit [Thermo Scientific, 24612]).

4.6 | Mass Spectrometry and Analysis of Samples

4.6.1 | Sample Preparation

Lysis buffer containing 10% sodium dodecyl sulfate (SDS) and 100 mM triethylammonium bicarbonate (TEAB) at pH 8.5 was added to the samples to a final concentration of 5% SDS and 50 mM TEAB. Proteins were reduced by adding 15 mM dithiothreitol, incubated for 30 min at 55°C, and alkylated by adding 30 mM iodoacetamide and incubating for 15 min at room temperature in the dark. Phosphoric acid was added to a final concentration of 2.75%, and the samples were subsequently diluted six-fold with a binding buffer containing 90% methanol in 100 mM TEAB, pH 7.55. After loading the samples onto S-trap microcolumns (Protifi) by centrifugation for 30 s at 4000 × *g*, the columns were washed three times with 150 μL binding buffer, and 1 μg trypsin in 20 μL was added for digestion overnight at 37°C. Peptides were eluted three times, first with 40 μL of 50 mM TEAB, then with 40 μL of 0.2% formic acid (FA) in water, and finally with 40 μL of 0.2% FA in water/acetonitrile (ACN) (50/50, v/v). Eluted peptides were entirely dried by vacuum centrifugation and redissolved in 100 μL loading solvent A (0.1% trifluoroacetic acid [TFA] in water/ACN [98:2, v/v]) for desalting in a reversed-phase (RP) C18 OMIX tip (Agilent). The tip was first washed three times with 100 μL pre-wash buffer (0.1% TFA in water/ACN [20:80, v/v]) and pre-equilibrated five times with 100 μL of wash buffer (0.1% TFA in water) before the sample was loaded on the tip. After peptide binding, the tip was washed three times with 100 μL of wash buffer, and peptides were eluted twice with 100 μL elution buffer (0.1% TFA in water/ACN [40:60, v/v]). The combined elutions were dried in a vacuum concentrator.

4.6.2 | LC–MS/MS Analysis and Identification and Quantification of Proteins

Peptides were re-dissolved in 20 μL loading solvent A (0.1% trifluoroacetic acid in water/acetonitrile ([ACN] 98:2, v/v) of which 15 μL was injected for LC–MS/MS analysis on an Ultimate 3000 RSLCnano system in-line connected to a Q Exactive HF mass spectrometer (Thermo). Trapping was performed at 10 μL/min for 2 min in loading solvent A on a 5 mm trapping column (Thermo Scientific, 300 μm internal diameter [I.D.], 5 μm beads). The peptides were separated on a 250 mm Waters nanoEase M/Z HSS T3 Column, 100 Å, 1.8 μm, 75 μm inner diameter (Waters Corporation), kept at a constant temperature of 45°C. Peptides were eluted by a non-linear gradient starting at 1% MS solvent B and reaching 33% MS solvent B (0.1% FA in water/acetonitrile [2:8, v/v]) in 100 min, 55% MS solvent B (0.1% FA in water/acetonitrile [2:8, v/v]) in 135 min, 70% MS solvent B in 145 min followed by a 10-min wash in 70% MS solvent B and re-equilibration with MS solvent A (0.1% FA in water). The mass spectrometer was operated in a data-dependent mode, automatically switching between MS and MS/MS acquisition for the 12 most abundant ion peaks per MS spectrum. Full-scan MS spectra (375–1500 m/z) were acquired at a resolution of 60,000 in the Orbitrap analyzer after accumulation to a target value of 3,000,000. The 12 most intense ions above the threshold value of 15,000 were isolated with a width of 1.5 m/z for fragmentation at a normalized collision energy of 30% after filling the trap at a target value of 100,000 for a maximum of 80 ms. MS/MS spectra (200–2000 m/z) were acquired at a resolution of 15,000 using an Orbitrap analyzer.

For protein identification and quantification, spectra were searched against the *Oryza sativa* (indica subspecies) genome sequence found in UniProt. After analysis of the mass spectrometry data, a total of 100,644 peptide-to-spectrum matches (PSMs) were performed, resulting in 6722 identified unique peptides corresponding to 1561 identified proteins. Further data analysis of the shotgun results was performed with an in-house R script using the protein groups output table from MaxQuant. Reverse database hits were removed, label-free quantification (LFQ) intensities were log2 transformed, and five biological replicate samples were grouped. Proteins with less than three valid values in at least one (biological) group were removed, and missing values were imputed from a normal distribution centered around the detection limit (package DEP) (44), leading to a list of 488 quantified proteins in the experiment, used for further data analysis. To compare protein abundance between pairs of sample groups (UV/infected vs. NoUV/infected, UV/non-infected vs. NoUV/non-infected, UV/non-infected vs. UV/infected and NoUV/non-infected vs. NoUV/infected sample groups), statistical testing for differences between two group means was performed, using the package limma (Ritchie et al. 2015). Statistical significance for differential regulation was set to a false discovery rate (FDR) of < 0.05 and $|\log2FC| = 2$. Data are available via ProteomeXchange with the identifier PXD045853. ZZ-scored LFQ intensities from significantly regulated proteins were plotted in a heatmap after non-supervised hierarchical clustering. Results are shown in Supplementary Figure S1.

Author Contributions

P.J.O., S.B., T.A., and K.G. planned and designed the study. P.J.O. performed experiments. P.J.O. and R.V.E. interpreted the data and wrote the original manuscript. S.B., G.O., T.A., and K.G. revised the paper. All authors read and approved the final manuscript.

Acknowledgments

We thank the team from VIB Proteomics Core, Ghent University, for their help in the sample preparation, mass spectrometry and bioinformatics analysis.

Conflicts of Interest

The authors declare no conflicts of interest.

Data Availability Statement

The datasets generated and/or analyzed during the current study are available in the PRIDE repository https://www.ebi.ac.uk/pride/archive/. The mass spectrometry proteomics data have been deposited to the ProteomeXchange Consortium via the PRIDE [1] partner repository with the dataset identifier: PXD045853 and:10.6019/PXD045853.

References

Albar, L., M. Bangratz-Reyser, E. Hébrard, M. N. Ndjiondjop, M. Jones, and A. Ghesquière. 2006. "Mutations in the eIF (iso)4G Translation Initiation Factor Confer High Resistance of Rice to *Rice Yellow Mottle Virus*." *Plant Journal* 47: 417–426.

Alcaide-Loridan, C., and I. Jupin. 2012. "Ubiquitin and Plant Viruses, Let's Play Together!" *Plant Physiology* 160: 72–82.

Bakker, W. "*Characterization and Ecological Aspects of Rice Yellow Mottle Virus in Kenya*".

Balzarini, S., R. Van Ende, A. Voet, and K. Geuten. 2023. "A Widely Applicable and Cost-Effective Method for Specific RNA–Protein Complex Isolation." *Scientific Reports* 13: 6898.

Bastet, A., C. Robaglia, and J.-L. Gallois. 2017. "eIF4E Resistance: Natural Variation Should Guide Gene Editing." *Trends in Plant Science* 22: 411–419.

Beckmann, B. M. 2017. "RNA Interactome Capture in Yeast." *Methods* 118-119: 82–92. https://doi.org/10.1016/j.ymeth.2016.12.008.

Bonneau, C., C. Brugidou, L. Chen, R. N. Beachy, and C. Fauquet. 1998. "Expression of the Rice Yellow Mottle Virus P1 Proteinin Vitroandin Vivo and Its Involvement in Virus Spread." *Virology* 244: 79–86.

Chaturvedi, S., K. Kalantidis, and A. L. N. Rao. 2014. "A Bromodomain-Containing Host Protein Mediates the Nuclear Importation of a Satellite RNA of Cucumber Mosaic Virus." *Journal of Virology* 88: 1890–1896.

Cléry, A., M. Blatter, and F. H.-T. Allain. 2008. "RNA Recognition Motifs: Boring? Not Quite." *Current Opinion in Structural Biology* 18: 290–298.

Darai, N., P. Mahalapbutr, P. Wolschann, V. S. Lee, M. T. Wolfinger, and T. Rungrotmongkol. 2022. "Theoretical Studies on RNA Recognition by Musashi 1 RNA-Binding Protein." *Scientific Reports* 12: 12137.

Davey, N. E., G. Travé, and T. J. Gibson. 2011. "How Viruses Hijack Cell Regulation." *Trends in Biochemical Sciences* 36: 159–169.

Dicker, K., A. I. Järvelin, M. Garcia-Moreno, and A. Castello. 2021. "The Importance of Virion-Incorporated Cellular RNA-Binding Proteins in Viral Particle Assembly and Infectivity." *Seminars in Cell and Developmental Biology* 111: 108–118. https://doi.org/10.1016/j.semcdb.2020.08.002.

Drugeon, G., and I. Jupin. 2002. "Stability in Vitro of the 69K Movement Protein of Turnip Yellow Mosaic Virus Is Regulated by the Ubiquitin-Mediated Proteasome Pathway." *Journal of General Virology* 83: 3187–3197.

Dubois, J., A. Traversier, T. Julien, et al. 2019. "The Nonstructural NS1 Protein of Influenza Viruses Modulates *TP53* Splicing Through Host Factor CPSF4." *Journal of Virology* 93, no. 7: 10-1128.

Fargette, D., A. Pinel, Z. Abubakar, et al. 2004. "Inferring the Evolutionary History of *Rice Yellow Mottle Virus* From Genomic, Phylogenetic, and Phylogeographic Studies." *Journal of Virology* 78: 3252–3261.

Fraser, C. S., and J. A. Doudna. 2007. "Structural and Mechanistic Insights Into Hepatitis C Viral Translation Initiation." *Nature Reviews. Microbiology* 5: 29–38.

Gao, L., W. Shen, P. Yan, D. Tuo, X. Li, and P. Zhou. 2012. "NIa-Pro of Papaya Ringspot Virus Interacts With Papaya Methionine Sulfoxide Reductase B1." *Virology* 434: 78–87.

Garcia-Moreno, M., M. Noerenberg, S. Ni, et al. 2019. "System-Wide Profiling of RNA-Binding Proteins Uncovers Key Regulators of Virus Infection." *Molecular Cell* 74: 196–211.e11.

Garcia-Ruiz, H. 2018. "Susceptibility Genes to Plant Viruses." *Viruses* 10: 484. https://doi.org/10.3390/v10090484.

Girardi, E., S. Pfeffer, T. F. Baumert, and K. Majzoub. 2021. "Roadblocks and Fast Tracks: How RNA Binding Proteins Affect the Viral RNA Journey in the Cell." *Seminars in Cell and Developmental Biology* 111: 86–100. https://doi.org/10.1016/j.semcdb.2020.08.006.

Gräwe, C., S. Stelloo, F. A. H. van Hout, and M. Vermeulen. 2021. "RNA-Centric Methods: Toward the Interactome of Specific RNA Transcripts." *Trends in Biotechnology* 39: 890–900.

Hafner, M., M. Landthaler, L. Burger, et al. 2010. "PAR-CliP—A Method to Identify Transcriptome-Wide the Binding Sites of RNA Binding Proteins." *Journal of Visualized Experiments* 41: 2034. https://doi.org/10.3791/2034.

Hébrard, E., A. Pinel-Galzi, and D. Fargette. 2008. "Virulence Domain of the RYMV Genome-Linked Viral Protein VPg Towards Rice rymv1–2-Mediated Resistance." *Archives of Virology* 153: 1161–1164.

Hébrard, E., N. Poulicard, C. Gérard, et al. 2010. "Direct Interaction Between the *Rice Yellow Mottle Virus* (RYMV) VPg and the Central Domain of the Rice eIF (iso)4G1 Factor Correlates With Rice Susceptibility and RYMV Virulence." *Molecular Plant-Microbe Interactions* 23: 1506–1513.

Hébrard, E., N. Poulicard, and M. Rakotomalala. 2021. "Rice Yellow Mottle Virus (Solemoviridae)." In *Encyclopedia of Virology*, 675–680. Elsevier. https://doi.org/10.1016/B978-0-12-809633-8.21244-2.

Huh, S. U., and K.-H. Paek. 2013. "Plant RNA Binding Proteins for Control of RNA Virus Infection." *Frontiers in Physiology* 4: 397.

Hyodo, K., M. Kaido, and T. Okuno. 2014. "Host and Viral RNA-Binding Proteins Involved in Membrane Targeting, Replication and Intercellular Movement of Plant RNA Virus Genomes." *Frontiers in Plant Science* 5: 321.

Imura, Y., M. Molho, C. Chuang, and P. D. Nagy. 2015. "Cellular Ubc2/Rad6 E2 Ubiquitin-Conjugating Enzyme Facilitates Tombusvirus Replication in Yeast and Plants." *Virology* 484: 265–275.

Köster, T., M. Reichel, and D. Staiger. 2019. "CLIP and RNA Interactome Studies to Unravel Genome-Wide RNA-Protein Interactions in Vivo in Arabidopsis thaliana." *Methods* 178: 63–71.

Lee, S., Y. S. Lee, Y. Choi, et al. 2021. "The SARS-CoV-2 RNA Interactome." *Molecular Cell* 81: 2838–2850.e6.

Li, Z., D. Barajas, T. Panavas, D. A. Herbst, and P. D. Nagy. 2008. "Cdc34p Ubiquitin-Conjugating Enzyme Is a Component of the Tombusvirus

Replicase Complex and Ubiquitinates p33 Replication Protein." *Journal of Virology* 82: 6911–6926.

LorkoviM, Z. J. 2002. "Genome Analysis: RNA Recognition Motif (RRM) and K Homology (KH) Domain RNA-Binding Proteins From the Flowering Plant Arabidopsis Thaliana." *Nucleic Acids Research* 30: 623–635.

Mäkinen, K. 2020. "Plant Susceptibility Genes as a Source for Potyvirus Resistance." *Annals of Applied Biology* 176: 122–129.

Maris, C., C. Dominguez, and F.H.-T. Allain. 2005. "The RNA Recognition Motif, a Plastic RNA-Binding Platform to Regulate Post-Transcriptional Gene Expression." *FEBS Journal* 272: 2118–2131.

Marondedze, C., L. Thomas, N. L. Serrano, K. S. Lilley, and C. Gehring. 2016. "The RNA-Binding Protein Repertoire of Arabidopsis thaliana." *Scientific Reports* 6: 1–13.

Martínez de Alba, A. E., R. Sägesser, M. Tabler, and M. Tsagris. 2003. "A Bromodomain-Containing Protein From Tomato Specifically Binds Potato Spindle Tuber Viroid RNA In Vitro and In Vivo." *Journal of Virology* 77: 9685–9694.

Masutani, M., N. Sonenberg, S. Yokoyama, and H. Imataka. 2007. "Reconstitution Reveals the Functional Core of Mammalian eIF3." *EMBO Journal* 26: 3373–3383.

McHugh, C. A., and M. Guttman. 2018. "RAP-MS: A Method to Identify Proteins that Interact Directly with a Specific RNA Molecule in Cells." *Methods in molecular biology (Clifton, N.J.)* 1649: 473–488. https://doi.org/10.1007/978-1-4939-7213-5_31.

Nagy, P. D., and J. Pogany. 2012. "The Dependence of viral RNA Replication on Co-Opted Host Factors." *Nature Reviews Microbiology* 10: 137–149. https://doi.org/10.1038/nrmicro2692.

Opalka, N., C. Brugidou, C. Bonneau, et al. 1998. "Movement of Rice Yellow Mottle Virus Between Xylem Cells Through Pit Membranes." *Proceedings of the National Academy of Sciences* 95: 3323–3328.

Opalka, N., M. Tihova, C. Brugidou, et al. 2000. "Structure of Native and Expanded Sobemoviruses by Electron Cryo-Microscopy and Image Reconstruction." *Journal of Molecular Biology* 303: 197–211.

Orjuela, J., E. F. T. Deless, O. Kolade, S. Chéron, A. Ghesquière, and L. Albar. 2013. "A Recessive Resistance to *Rice Yellow Mottle Virus* Is Associated With a Rice Homolog of the *CPR5* Gene, a Regulator of Active Defense Mechanisms." *Molecular Plant-Microbe Interactions* 26: 1455–1463.

Pidon, H., S. Chéron, A. Ghesquière, and L. Albar. 2020. "Allele Mining Unlocks the Identification of RYMV Resistance Genes and Alleles in African Cultivated Rice." *BMC Plant Biology* 20: 222.

Pinel-Galzi, A., E. Hébrard, O. Traoré, D. Silué, and L. Albar. 2018. "Protocol for RYMV Inoculation and Resistance Evaluation in Rice Seedlings." *Bio-Protocol* 8: e2863.

Queiroz, R. M. L., T. Smith, E. Villanueva, et al. 2019. "Comprehensive Identification of RNA–Protein Interactions in any Organism Using Orthogonal Organic Phase Separation (OOPS)." *Nature Biotechnology* 37: 169–178.

Raabe, K., D. Honys, and C. Michailidis. 2019. "The Role of Eukaryotic Initiation Factor 3 in Plant Translation Regulation." *Plant Physiology and Biochemistry* 145: 75–83.

Reichel, C., and R. N. Beachy. 2000. "Degradation of Tobacco Mosaic Virus Movement Protein by the 26S Proteasome." *Journal of Virology* 74: 3330–3337.

Reichel, M., Y. Liao, M. Rettel, et al. 2016. "In Planta Determination of the mRNA-Binding Proteome of Arabidopsis Etiolated Seedlings." *Plant Cell* 28: 2435–2452. https://doi.org/10.1105/tpc.16.00562.

Ritchie, M. E., B. Phipson, D. Wu, et al. 2015. "Limma Powers Differential Expression Analyses for RNA-Sequencing and Microarray Studies." *Nucleic Acids Research* 43: e47.

Schepetilnikov, M., K. Kobayashi, A. Geldreich, et al. 2011. "Viral Factor TAV Recruits TOR/S6K1 Signalling to Activate Reinitiation After Long ORF Translation." *EMBO Journal* 30: 1343–1356.

Schmidt, N., C. A. Lareau, H. Keshishian, et al. 2021. "The SARS-CoV-2 RNA–Protein Interactome in Infected Human Cells." *Nature Microbiology* 6: 339–353.

Shen, Q., T. Hu, M. Bao, et al. 2016. "Tobacco RING E3 Ligase NtRFP1 Mediates Ubiquitination and Proteasomal Degradation of a Geminivirus-Encoded βC1." *Molecular Plant* 9: 911–925.

Swatek, K. N., and D. Komander. 2016. "Ubiquitin Modifications." *Cell Research* 26: 399–422.

Thiébeauld, O., M. Schepetilnikov, H. S. Park, et al. 2009. "A New Plant Protein Interacts With eIF3 and 60S to Enhance Virus-Activated Translation Re-Initiation." *EMBO Journal* 28: 3171–3184.

Trendel, J., T. Schwarzl, R. Horos, et al. 2019. "The Human RNA-Binding Proteome and Its Dynamics During Translational Arrest." *Cell* 176: 391–403.e19.

Urdaneta, E. C., and B. M. Beckmann. 2019. "Fast and Unbiased Purification of RNA-Protein Complexes After UV Cross-Linking." *Methods* 178: 72–82. https://doi.org/10.1016/j.ymeth.2019.09.013.

Urdaneta, E. C., C. H. Vieira-Vieira, T. Hick, et al. 2019. "Purification of Cross-Linked RNA-Protein Complexes by Phenol-Toluol Extraction." *Nature Communications* 10: 1–17.

Van Ende, R., S. Balzarini, and K. Geuten. 2020. "Single and Combined Methods to Specifically or Bulk-Purify RNA–Protein Complexes." *Biomolecules* 10: 1–27.

Van Schie, C. C. N., and F. L. W. Takken. 2014. "Susceptibility Genes 101: How to Be a Good Host." *Annual Review of Phytopathology* 52: 551–581.

Verchot, J. 2016. "Plant Virus Infection and the Ubiquitin Proteasome Machinery: Arms Race Along the Endoplasmic Reticulum." *Viruses* 8: 314.

Wagenmakers, A. J. M., R. J. Reinders, and W. J. Van Venrooij. 1980. "Cross-Linking of mRNA to Proteins by Irradiation of Intact Cells With Ultraviolet Light." *European Journal of Biochemistry* 112: 323–330.

Walker, P. J., S. G. Siddell, E. J. Lefkowitz, et al. 2021. "Changes to Virus Taxonomy and to the International Code of Virus Classification and Nomenclature Ratified by the International Committee on Taxonomy of Viruses (2021)." *Archives of Virology* 166: 2633–2648.

Walter, B. L., T. B. Parsley, E. Ehrenfeld, and B. L. Semler. 2002. "Distinct Poly (rC) Binding Protein KH Domain Determinants for Poliovirus Translation Initiation and Viral RNA Replication." *Journal of Virology* 76: 12008–12022.

Yassi, M. N. A., C. Ritzenthaler, C. Brugidou, C. Fauquet, and R. N. Beachy. 1994. "Nucleotide Sequence and Genome Characterization of Rice Yellow Mottle Virus RNA." *Journal of General Virology* 75: 249–257.

Supporting Information

Additional supporting information can be found online in the Supporting Information section.